Journal of South American Earth Sciences 104 (2020) 102932

Contents lists available at ScienceDirect

Journal of South American Earth Sciences

journal homepage: www.elsevier.com/locate/jsames

Slab flattening and tractional coupling drove Neogene clockwise rotation of Chiapas Massif, Mexico: Paleomagnetism of the Eocene El Bosque Formation

Roberto S. Molina-Garza [a,*], James Pindell [b], Paola Catalina Montaño Cortés [c]

[a] Centro de Geociencias, Universidad Nacional Autónoma de México, Campus Juriquilla, 76230, Mexico
[b] Tectonic Analysis Ltd., Chestnut House, Duncton, West Sussex, GU28 0LH, United Kingdom
[c] Corporación Geológica Ares, Bogotá, Colombia

ARTICLE INFO

Keywords:
Paleomagnetismo
Southern Mexico
Eocene
Miocene
Sierra chiapas
Tractional coupling
Flat slab

ABSTRACT

Dual-polarity characteristic magnetizations in red sandstones of the Early and Middle Eocene El Bosque Formation in central Chiapas, Mexico (D = 9.3° I = 23.6°; N = 19 selected sites, k = 32.6, α_{95} = 6.0°) indicate about 20° of clockwise rotation when compared with a coeval paleomagnetic reference pole in the North America craton. We interpret the rotation to result from traction between the base of the Chiapas Massif lithosphere and the low-angle subducting Cocos Plate. The northwest end of the massif overlies a shallower portion of the Cocos plate interface than the southeast end, which implies a greater amount and longer period of tractional coupling between the two plates in the northwest. We judge that the downdip, steep limb of the Cocos slab (beneath Gulf of Mexico) lies roughly in the regional mantle or hotspot reference frame. Assessments of Neogene North America-hotspot relative motion indicate an azimuth of ENE-WSW at 20 mm/yr, and thus we envisage that (1) the flat slab zone has been caused by the WSW telescoping of North America across the former geometry of the Cocos Benioff Zone, and (2) that the WNW end of the massif has undergone most tractional coupling with Cocos Plate than the ESE end. In turn, because the massif appears to have behaved as a rigid, unbroken body, this greater coupling has induced clockwise rotation that has been transferred as near-field shortening into the adjacent Sierra de Chiapas foldbelt.

1. Introduction

Sierra de Chiapas is an arcuate E-W to NW-SE trending Neogene fold and thrust belt system developed north of the Chiapas Massif in the Mexican states of Chiapas, Tabasco, and Veracruz, in the Bay of Campeche in the southern Gulf of Mexico, and in westernmost Guatemala (Dengo, 1969) (Fig. 1). The Sierra de Chiapas foldbelt is located in the back-arc region of the Late Miocene Chiapanecan arc, although since 9 Ma arc magmatism has migrated some 150 km into the foldbelt itself. It is a thin-skin foldbelt characterized by open folds, east-west trending sinistral strike-slip faults, and small-scale mainly north-vergent thrusts (Meneses-Rocha, 1985; Mandujano-Velásquez and Keppie, 2009). From regional seismic sections, shortening is estimated at ~60 km (Garcia-Molina, 1995) with greater shortening in the southwest and less shortening in the northeast (Mandujano-Velásquez and Keppie, 2009).

The driver of shortening in Sierra de Chiapas is not fully understood, but is usually inferred to be the result of poorly constrained basement shortening between Chiapas Massif and the Libertad Arch of the Yucatán or Maya Block (Fig. 1). The region lies within a broad triple junction between the Caribbean - North America - Cocos plates, leading to complex tectonic relations. Shortening has been related to transpression along the Caribbean-North America plate margin (e.g., Witt et al., 2012; Molina-Garza et al., 2015), but these models do not explain only Neogene shortening (Mandujano-Velásquez and Keppie, 2009) given the long and extended interaction between the Chortís Block and the southern Mexico margin suggested by plate reconstructions (Paleogene-Neogene according to Pindell et al. (1988). Mandujano-Velásquez and Keppie (2009) followed Couch and Woodcock (1981) who proposed shortening is driven by collision of a segment of the Tehuantepec Ridge with the Middle America Trench, inducing short-lived deformation on the hanging wall of the subduction zone. Molina-Garza et al. (2015) showed that shortening associated with transpression occurred along

* Corresponding author.
E-mail address: rmolina@geociencias.unam.mx (R.S. Molina-Garza).

https://doi.org/10.1016/j.jsames.2020.102932
Received 13 April 2020; Received in revised form 18 August 2020; Accepted 28 September 2020
Available online 15 October 2020
0895-9811/

the Tonalá shear zone south of the Chiapas Massif, but this occurred at or after about 10 Ma and (apparently) is not directly related to shortening in Sierra Chiapas foldbelt. Pindell and Miranda (2011) suggested that shortening was triggered by the eastward-migrating onset of subduction in the wake of the migrating Chortís Block, rather than by the passage of Chortís itself.

We sampled the Eocene El Bosque Formation, a series of continental red shales, sandstones and conglomerates in central Chiapas State to test with paleomagnetic data the hypothesis that the Chiapas Massif may have acted as an indenter in the origin of Sierra de Chiapas foldbelt. Our results suggest that clockwise rotation of the massif accompanied overall Neogene shortening in the Chiapas Foldbelt, suggesting a rotation pole somewhat to the southeast of the massif.

1.1. Geologic setting

The Sierra de Chiapas foldbelt includes three distinct geomorphic provinces north of the Chiapas Massif, and two fold systems in the subsurface. In the south of the foldbelt, the Sierra Monocline (Meneses-Rocha, 2001) includes gently north dipping Jurassic to Eocene strata (Fig. 1). The reverse fault province in the northeast of the foldbelt includes Cretaceous to Middle Miocene strata folded and affected by doubly verging thrust faults. The strike-slip province in the northwest is characterized by abrupt topographic changes. Two major strike-slip fault systems can be recognized, the Los Tuxtla-Malpaso system and the Altos de Chiapas system (highlands system). La Venta-Grijalva fault, north of the Chiapas Massif, is associated with a strong lineament in the aeromagnetic map of Chiapas. The east-west trending left-lateral strike slip faults of the highlands system post-date the main folding event in the foldbelt, and may accommodate as much as 70 km of displacement in various faults with minor displacement of a few km each (Meneses-Rocha, 2001; Witt et al., 2012). In addition, two folding provinces are buried by Late Miocene and younger siliciclastic strata, one straddling the Tabasco coast line (Reforma-Macuspana Basin) and the other in the Sonda de Campeche offshore (Comalcalco Basin; Fig. 1). According to seismic data (Mandujano-Velásquez and Keppie, 2009) a Cretaceous to Middle Miocene succession lies folded under a basin-wide pre-Tortonian (early Late Miocene) unconformity; folding culminated between 13 and 11 Ma (late Middle Miocene). A large portion of the foldbelt is buried under Upper Miocene to Quaternary siliciclastic strata, where it is of great hydrocarbon exploration significance.

The Mesozoic stratigraphy of the Sierra de Chiapas (Fig. 2) begins

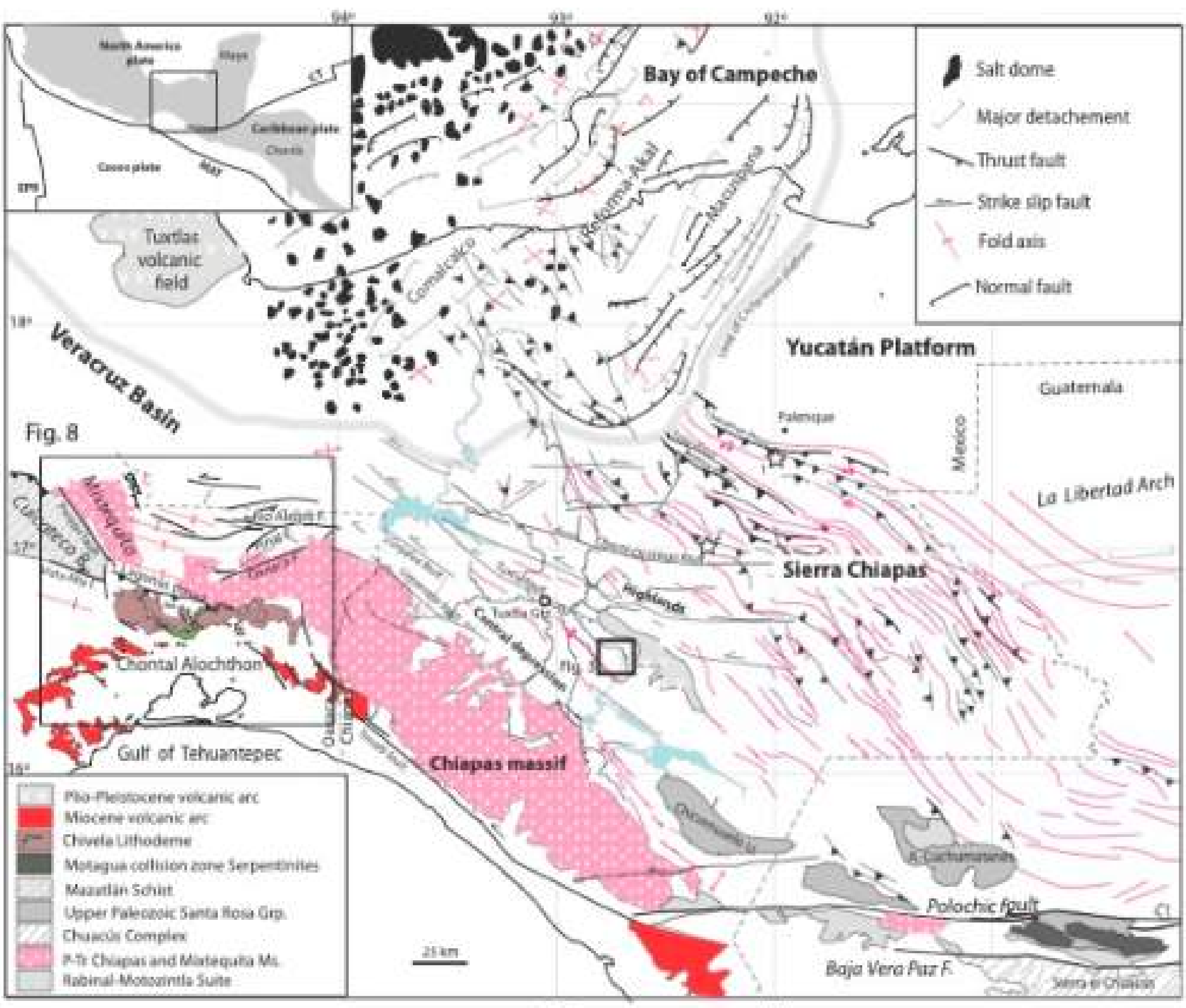

Fig. 1. Schematic tectonic map of southeast Mexico and part of Guatemala, after Garcia-Molina (1995), Meneses-Rocha (2001), and Ratschbacher et al. (2009).

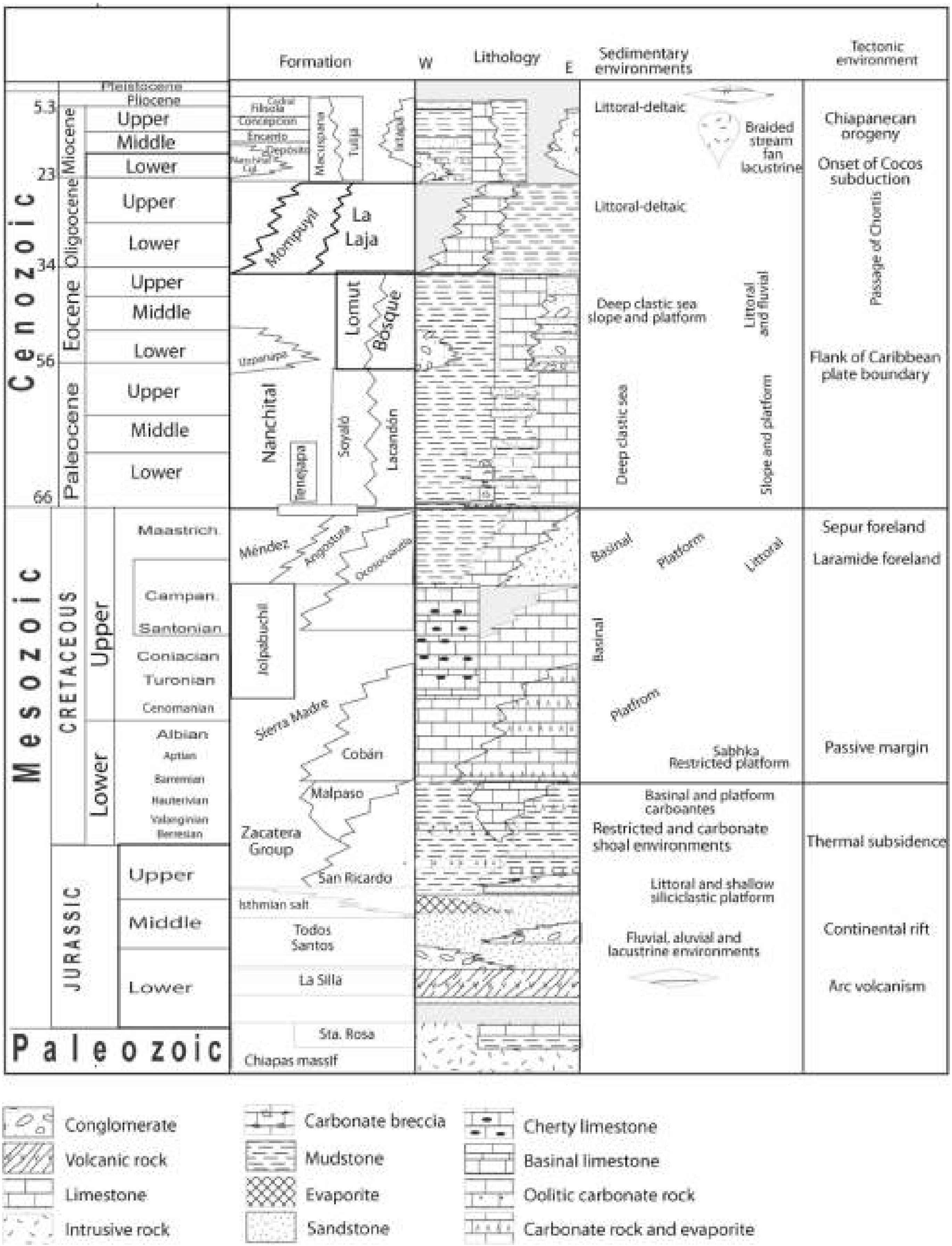

Fig. 2. Annotated stratigraphic column of Sierra Chiapas, modified from Mandujano-Velásquez (1996) and Villagomez and Pindell (2020).

with synrift continental deposits of the Todos Santos Group overlain by an Upper Jurassic transgressive succession included in the San Ricardo Formation (Blair, 1987; Godínez-Urban et al., 2011; Molina-Garza et al., 2020). In much of the foldbelt, evaporites were deposited over or interfingering with the Todos Santos Group, heralding the San Ricardo transgression, and have been drilled in eastern Sierra de Chiapas (Chávez-Valois, 1997). The evaporites are believed to have acted as the main detachment level for the folding (Mandujano-Velásquez and Keppie, 2009). The Cretaceous section includes the Sierra Madre Group (Quezada-Muñetón, 1987), a carbonate platform developed over inherited basement architecture from the earlier synrift phase. The northeastern domain of the Sierra Madre platform consists of the Aptian-Santonian Cobán restricted platform succession with various sabkha intervals (Chávez-Valois, 1997; Fourcade et al., 1999). The Upper Cretaceous Angostura Formation (and Campur Formation in Guatemala) records partial drowning of the platform during Campanian-Maastrichtian (Cros et al., 1998), so that uppermost Cretaceous strata include a mixed carbonate and terrigenous succession that deepens gradually northwards in Chiapas. North of the Chiapas Massif, Upper Cretaceous strata are assigned to the Angostura, Ocozocuautla, Xochitlán, and Méndez Formations that represent lateral facies changes recording progressively deeper depositional environments. The upward-deepening of the Sierra Madre platform and the change in sedimentation from carbonate to mixed carbonate and siliciclastics has been attributed variably to the Mexican "Laramide" orogeny and to tectonics in the Motagua collision zone (Pindell and Dewey, 1982; Rosenfeld, 1993; Meneses-Rocha, 2001). The Paleogene succession is predominantly terrigenous, especially in the western sector of the foldbelt. Tectonically driven subsidence led to deposition of the siliciclastic Paleocene Soyaló Formation in submarine fan systems in central Chiapas, and the Nanchital shale farther north and northwest. However, Paleocene strata in northeast and north central Chiapas correspond to carbonate deposition of the Lacandón and Tenejapa Formations (Vinson, 1962; Quezada-Muñetón, 1987). The Nanchital turbidite section includes the conspicuous pebble to boulder sized serpentinite bearing Eocene Uzpanapa marine conglomerate (Molina-Garza et al., 2019a). The Soyaló Formation is overlain in transitional contact in the Sierra de Chiapas monocline (Meneses-Rocha, 2001) by the littoral to continental El Bosque Formation, suggesting that the Soyaló basin became overfilled. North of the Malpaso fault, marine sedimentation is continuous throughout the Eocene-Miocene interval, including the Lomut, Mompuyil, Laja, Depósito and Tulijá Formations (Fig. 2); all units are dominated by sandstone, shale, and conglomerate deposited in shallow to littoral, slope, and deep-water environments that prograded north.

Miocene magmatism is widespread onshore in the Tehuantepec Isthmus, south of the Chiapas Massif, with ages ranging between 20 and 12 Ma along western Gulf of Tehuantepec, and ages between 11 and 9 Ma in Chiapas (along eastern Gulf of Tehuantepec) where they are associated with the Tonalá shear zone (Molina-Garza et al., 2015). Subduction magmatism extended south into the Chortís block (Padre Miguel suite, Molina-Garza et al., 2012). Magmatism migrated north from coastal Chiapas to the Altos region of central Chiapas in the Pliocene, with an apparent gap in magmatism between about 9 and 3 Ma (Garduño-Monroy et al., 2015) during the migration. In contrast to Oaxaca coast west of Tehuantepec (Keppie et al., 2012), the forearc has not been removed from offshore Chiapas State, where it includes the Tehuantepec terrane of Pindell and Miranda (2011), which we now believe comprises accreted arc basement of the western, trailing tail of the Chortis Block. Pliocene to recent magmatism occurred about 350 km from the trench in the Altos region (Chiapas highlands), suggesting the continuation of the eastward migration of slab flattening in Chiapas during Late Miocene to Present time (Pindell and Miranda, 2011). The diachronous flattening of the slab along the trench may have caused regional basement uplift reflected by the post-10 Ma uplift and exposure of the granitic Chiapas Massif complex (Villagomez and Pindell, 2020).

El Bosque Formation consists of pebble to cobble conglomerate, fine to coarse-grained sandstone, and mudstone deposited in fluvial and littoral environments (Ferrusquía-Villafranca et al., 2000). The El Bosque is not fossiliferous, but based on the presence of *Pellatispirella matleyi, Eoconuloides wellsi, Rothalia* sp.*, Rothalia hensoni, Camagueyia perplexa, Quinqueloculina* sp.*, Spiroloculina* sp.*, Arenagula* sp.*,* and *Valvulamina* sp. this unit is assigned to the Early-Middle Eocene (Islas-Tenorio et al., 2005; Vega et al., 2008). A single-grain zircon U–Pb maximum depositional age of 59.4 ± 1.7 Ma was reported by Witt et al. (2012).

We recognized the El Bosque Formation in central Chiapas as composed of thick to massive quartz-pebble to cobble conglomerate beds, red in color, intercalated with fine to medium red sandstone, purplish red siltstone and reddish orange sandstone lenses. Conglomerate beds are generally matrix-supported, and often conglomerate beds fine upward to fine sandstone; most conglomerate beds contain erosional bases. Clasts in the conglomerate are mostly quartz (white vein quartz), with some metamorphic and sedimentary lithic grains. We notice that there are no granite clasts in El Bosque Formation. Sandstones are lithic, moderately sorted, and often include grains 0.5–2 mm in size of vein quartz; common sedimentary structures include trough cross-bedding. Along the central Chiapas Depression (Fig. 1), El Bosque strata dip to the northeast 4–29° in an apparent open synform where the youngest strata are of Eocene age. An anastamosing or braided fluvial system is interpreted as the environment of deposition of El Bosque in this region. We also notice from inspection of geologic maps, such as Servicio Geológico Mexicano (2005) that there are no regional structural or tectonic discontinuities between the central Chiapas Depression and the Chiapas Massif.

2. Methods and sampling

We sampled the El Bosque Formation for paleomagnetic analysis, collecting mostly along the road from Chiapa de Corzo to Alcalá, as well as near the town of 20 de Noviembre, both in the Chiapas central depression east of Tuxtla Gutiérrez (Fig. 3). In general, outcrops of El Bosque are in low-lying areas in the hills along the Grijalva river valley; access to the most extensive exposures is limited by the river channel. We collected a total of 25 sites. Samples were drilled in the field with a gas-powered portable drill, with an average of about 10 samples per site. The samples were oriented with magnetic and solar compasses and an inclinometer. Twenty-four of the sites were collected in the El Bosque Formation, and one in the underlying Soyaló Formation. The El Bosque samples are red medium to fine-grained sandstones, hematite cemented (effectively redbeds). Samples were labelled ACA or NOV, for locations near Alcalá and 20 de Noviembre, respectively. Sampling coordinates, structural data and lithologic observations are in Table 1 of Supplementary Material. All sites were collected only on the northeast dipping flank of the regional Grijalva syncline because of access restrictions.

The samples were prepared into standard cylinders 2.1 by 2.5 cm with a non-magnetic blade. The NRM was measured with a JR-6 spinner magnetometer (AGICO Instruments, Brno, Czech Republic), and samples were subjected to progressive thermal demagnetization with an ASC Scientific thermal demagnetizer. The vectorial composition of the NRM was interpreted from orthogonal demagnetization diagrams (Zijderveld, 1967). The direction of the components was calculated using principal component analysis (Kirschvink, 1980). Site and formation means used Fisher's statistics (Fisher, 1953). IRM (Isothermal Remanent Magnetization) acquisition curves obtained with a pulse magnetizer, and high temperature thermomagnetic curves acquired in a home-built Curie balance, were used to characterize the magnetic mineralogy. The anisotropy of magnetic susceptibility was determined with a KLY-3 Kappabridge (Brno, Czech Republic).

3. Results

The natural remanent magnetization (NRM) of samples of El Bosque

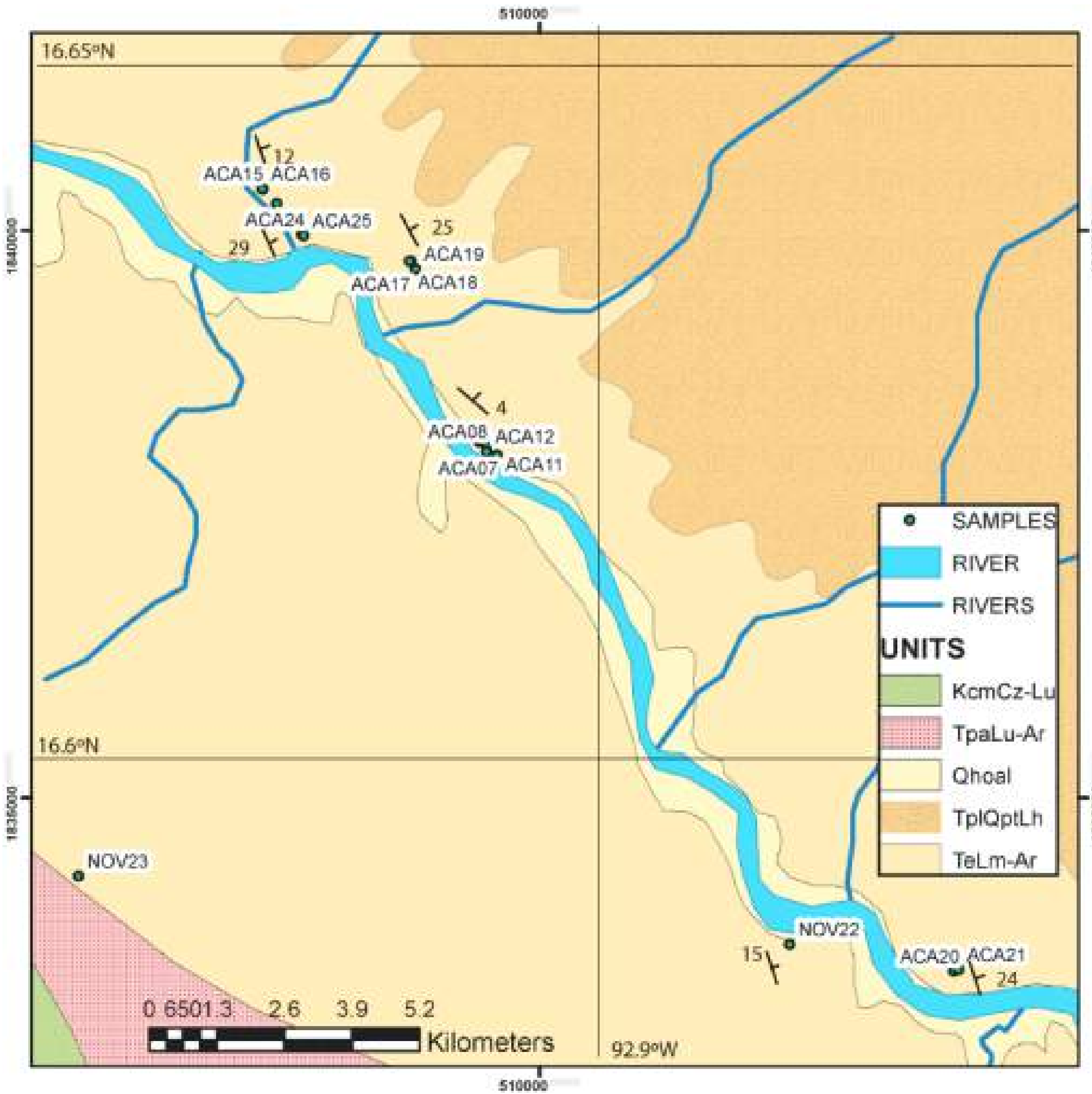

Fig. 3. Paleomagnetism sampling site location. Sites in the Bosque Formation are south and east of Tuxtla Gutiérrez in the municipalities of Alcalá and 20 de Noviembre over a geologic map (modified from Servicio Geológico Mexicano, 2005).

Formation is moderately low, averaging about 10 mA/m. We observed both near univectorial and multi-component behaviors in demagnetization experiments. Generally, the NRM decays in univectorial fashion with well-defined linear demagnetization trajectories to the origin (Fig. 4A, C and 4F). The magnetization is of distributed unblocking temperatures in excess of 600 °C and generally of high coercivity in excess of 90 mT. The magnetization is north directed and of moderate positive inclination or its antipodal (Fig. 4F). In some samples two magnetization components were observed. A low laboratory unblocking temperature north-directed magnetization sometimes overprints a higher stability component; the low temperature overprint has maximum unblocking temperature and maximum coercivity 180 °C and 20 mT, respectively (Fig. 4B and D) and the high-stability magnetization is south-directed and of moderate negative inclination. In a minority of samples AF demagnetization defines linear trajectories to the origin (Fig. 4E). The dual polarity, high stability component is considered the characteristic magnetization (ChRM).

The ChRM is generally hard, and about 50% of the NRM is unblocked at laboratory temperatures of about 600 °C in some samples (Fig. 4C and D), but distributed unblocking temperatures between about 200 and 620 °C typical of fine-grained pigmentary hematite are more common (Fig. 4A, C and 4F). For several samples with south-directed characteristic magnetizations AF and thermal fail to fully isolate this component, and we were forced to combine great circles and stable end points using the method of Bailey and Halls (1984) (Fig. 4G and H). Maximum laboratory unblocking temperatures in excess of 600 °C and high coercivity

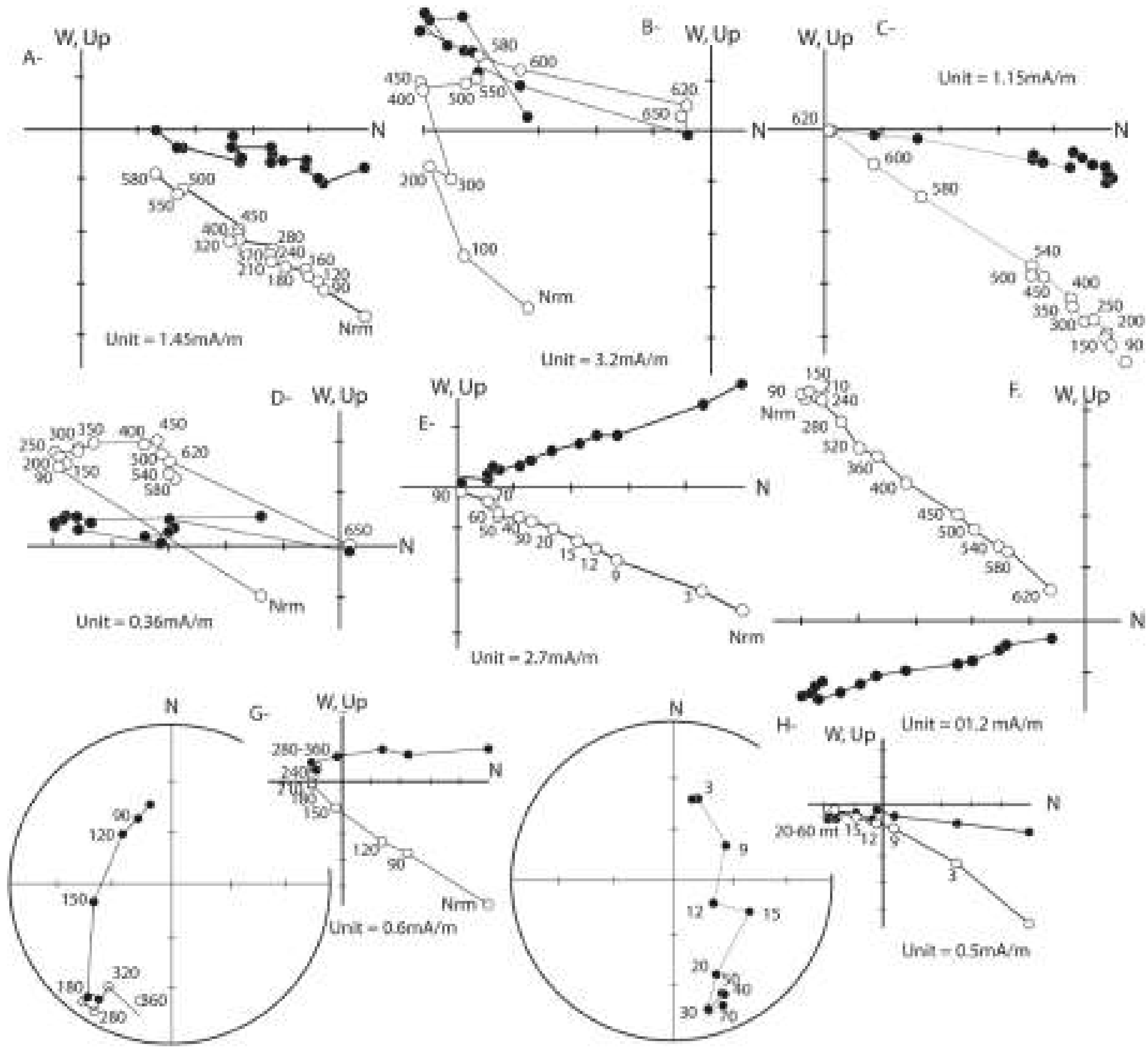

Fig. 4. (A–F) Orthogonal demagnetization diagrams for selected samples of the El Bosque Formation. Solid (open) symbols correspond to the projection of the horizontal (vertical) component. (G–H) Are examples of demagnetization diagrams and stereographic projection of demagnetization trajectories for a site that required the combination of great circles and stable end point directions.

indicate that the ChRM resides, at least in part, in hematite. But AF demagnetization results suggest that magnetite is also present, and in several sites (ACA17, ACA18, and ACA20) the ChRM is defined by AF demagnetization in the range from 15 to 60 mT and laboratory unblocking temperatures <360 °C (Fig. 4E). These sites also display higher bulk susceptibility. The IRM acquisition curve is dominated by the soft magnetic phase, but most samples do not reach saturation with induction of 3 T.

Site mean directions are relatively well determined with k–values generally greater than 20 (smaller in 7 of 27 site means) and a minimum of 4 samples (Table 1 and Fig. 5). Eleven sites record normal polarity (north directed and positive inclination), fourteen are of reverse polarity, and two sites record mixed polarity (a mean was calculated for each polarity). The angle between the mean of normal polarity sites and the (inverted) mean of reverse polarity sites is 1.8°, passing a test for antipodality with an A classification (McFadden and McElhinny, 1990). The precision parameter decreases slightly upon application of a tilt correction, from 38.2 to 33.4. The decrease is not statistically significant. If the DC fold test (Enkin, 2003) is applied with seven “limbs” corresponding to sites from the same seven localities sharing the same bedding, the best fitting slope is obtained with 125.7% unfolding but the test is still indeterminate. Between-site dispersion is also relatively low, but the mean calculated includes 8 site means with poor statistics ($k<16$ and $\alpha_{95}>20°$). A better estimate of the overall formation mean is of Dec = 9.3° and Inc = 23.6° (N = 19, k = 32.6, and α_{95} = 6°). We used 175 sample directions (Fig. 5C) and applied the Elongation/Inclination method to estimate eccentricity and the best estimate of flattening required to correct the observed inclination following the model of Tauxe and Kent (2004). This analysis resulted in an estimated flattening value (f) of 0.67 and a mean inclination of 34.7° (95% confidence Limits: 29.4°, 40.3°).

The bulk magnetic susceptibility is relatively low, of the order of ~50 E−06 SI (Supplemental Material Table 2), but it is high at sites ACA17, 18, 19 and 20 where it is of the order of ~1–5 E−03 SI. The majority of the sites studied are characterized by type 1 (sedimentary) oblate fabrics (T > 0), with minimum susceptibility axis k_3 near vertical and k_1-k_2 susceptibility axes in distributed near the horizontal plane. The fabric is relatively well developed, with percent anisotropy values between 1.03 and 1.118, except for site ACA16 where it is higher (1.31). The susceptibility axes define a magnetic foliation plane that deeps gently to the WSW (Fig. 6).

The thermomagnetic experiments (Ms vs. T), conducted in air, reveal

Table 1
Paleomagnetic data and statistical parameters.

Sites	Rango mT y °C	DD/dip	n/nc	IN SITU		TILT CORRECTED		k	α95
				DEC	INC	DEC	INC		
ACA01	100–580 °C distributed	58/6	6/10	19.1	30.7	21.1	26.0	24.6	13.8
ACA02	hard, 100–580 °C, distrib.	55/4	4/4	22.5	16	23.0	12.6	15.3	15.3
ACA03	hard, 200–580 °C	55/4	6/10	178.6	−13.2	179.3	−11	18.5	16
ACA04r	>300 °C	55/4	6/10	190.2	−22	191.1	−19.1	23.1	14.2
ACA04n	300–650 °C	55/4	3/10	31.9	41.5	33.2	37.8	7.2	49.8
ACA05	>580 °C	55/4	5/10	195.9	−34.2	197.5	−31.1	14.1	21.1
ACA06	350–620 °C	55/4	5/10	6.1	37.3	0.3	34.6	12.5	19.7
ACA07	400–650 °C	55/4	11/12	3.4	33.7	5.4	31.2	75.7	5.3
ACA08	450–650 °C	55/4	8/8	7.1	28.5	8.6	25.8	15.4	15.9
ACA09	240–620 °C, distributed	55/4	9/12	355.8	31.8	357.8	29.7	28.1	9.9
ACA10	>70mT/>280 °C	55/4	5/14	174.3	−29.7	176.2	−27.7	12.4	22.6
ACA11	500–650 °C	40/19	12/12	359.1	35.4	5.3	20.3	69.2	5.3
ACA12	200–650 °C	40/19	8/9	173.6	−22.1	177.3	−8.5	44.6	8.4
ACA13	>80 mT, 600–680 °C	74/12	8/10	186.1	−61.1	202.8	−54.9	48.3	8.1
ACA14	300–650 °C	74/12	10/10	178.2	−35.9	185.9	−32.2	80.7	5.4
ACA15	200–580 °C	74/12	8/10	182.5	−35.6	189.8	−31.0	91.5	5.8
ACA16	>80 mT, 300–580 °C	74/12	8/10	169.1	−42.8	179.7	−40.6	29.4	10.4
ACA17	MDF 15–20 mT	60/25	6/10	357.4	32.6	7.7	18.9	57.2	8.9
ACA18	15–20 mT, ~300 °C	60/25	9/10	353.1	27.9	2.2	16.1	44.4	7.8
ACA19r	>80 mT, >300 °C	60/25	4/10	175.2	−30.7	184.9	−17.5	55.7	12.4
ACA19n	~300 °C	60/25	4/10	344.8	32.4	357.3	23.2	24.5	18.9
ACA20	AF20, max T 450 °C	72/24	9/10	16.5	24.8	22.6	10.8	49.7	7.4
ACA21	AF>15, max T 450 °C, GC	72/24	5/10	193.9	−31.9	202.9	−17.5	13.2	18.8
11/22	0–70 mT	70/15	8/9	4.7	34.1	12.5	26.9	41.9	8.7
11/23	GC, 280 °C	66/29	8/10	193.4	−27.2	202.3	−11.6	55.2	9.3
ACA24	0–330 °C GC	65/29	3/10	171.2	−24.7	182.7	−18.5	39.3	19.9
ACA25	100–480 °C GC	65/29	4/10	176.6	−24.4	187.0	−15.8	21.2	17.6

Mean all N = 27	**Dec**	**Inc**	**k**	**α95**	Sample mean Dec = 8.9°, Inc = 25.9°, α95 = 2.6°, k = 17.75, n = 175
Mean Insitu	3.6	31.6	38.2	4.6	Normal sites Dec = 10.5, Inc = 24.4, k = 39.4, α95 = 6.7, N = 13
Mean Tilt	9.3	24.4	33.4	4.9	Reverse sites Dec = 188.2, Inc = −24.2, k = 27.6, α95 = 7.7, n = 14
Selected α95 < 16	**Dec**	**Inc**	**k**	**α95**	Bootstrap Median Inclination = 34.4°, 95% Confidence Limits: 29.4°, 40.2°
N = 19	9.3	23.6	32.6	6.0	Bootstrap Median flattening factor (f) = 0.67, 95% Confidence Limits: 0.53, 0.82

Table 1. Paleomagnetic dadta and statistical parameters for the El Bosque Formation, Chiapas. Range is the demagnetization inverval of the ChRM. DD and Dip and re dip direction and dip; n/nc number of samples used/collected; dec = declination; inc = inclination; k and apha 95 are the statistical parameters (Fisher, 1953).

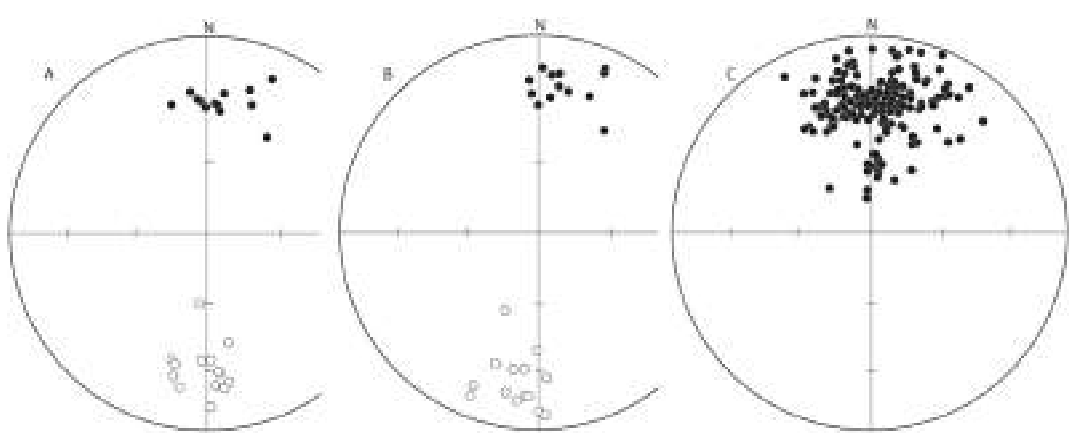

Fig. 5. Equal area stereographic projection of in situ site means (A), tilt corrected site means (B), and individual sample directions (C). Open (closed) symbols are upper (lower) hemisphere projections corresponding to negative (positive) inclinations.

some changes to the magnetic mineralogy over elevated temperature intervals. Heating curves are reversible or partially reversible upon cooling, indicating only slight changes in the magnetic mineralogy during heating. Curves indicate principal Curie temperatures at about 580 °C and about 680 °C, corresponding to pure magnetite and hematite, respectively.

3.1. *Interpretation*

The ChRM is interpreted as a primary remanence residing in hematite. Distributed unblocking temperatures are interpreted to reflect a remanence residing in pigmentary hematite, with small contributions from specular hematite in some samples. For sites where the remanence is defined by AF demagnetization we interpret the ChRM as a depositional remanence residing in detrital magnetite. The presence of dual polarity magnetizations, the site-mean angular dispersion, and the stratigraphy suggest that secular variation was adequately averaged.

The mean paleomagnetic declination observed in El Bosque Formation is of 9.3° and the corrected inclination I = 34.7° (α_{95} = 6.0°). The mean direction passes a reversal test, it is thus interpreted to represent

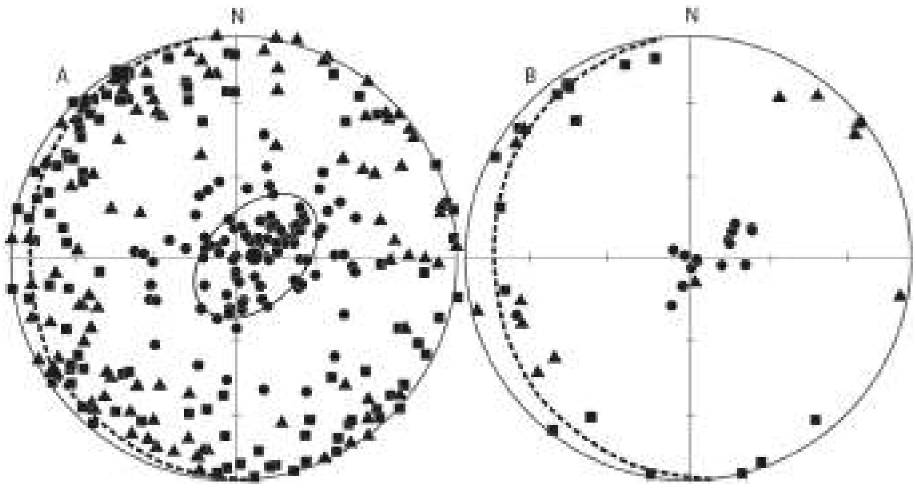

Fig. 6. (A) Equal area projection of principal susceptibility axes for specimens of the El Bosque Formation (maximum squares, intermediate triangle, and minimum circles) with mean magnetic foliation plane and mean of k_{min} with confidence interval. (B) Same as A, but site mean directions.

the time-average-paleomagnetic field at the time of deposition of this unit and validates its use for tectonic interpretations. We compared the overall mean of El Bosque Formation with the expected reference direction calculated using a pole at 80°N-175°E, a reference pole position for 50 Ma for North America of Torsvik et al. (2012) with a weighted average uncertainty of 4.0°. The expected direction is of D = 346.9° I = 31.9° from which we calculate R and F values of +22.4° ± 6.1° and +2.8° ± 7.1°, respectively; this indicates statistically significant clockwise rotation and no discernible latitudinal displacement. We infer that clockwise rotation applies to the entire Chiapas Massif, because outcrop patterns in the Chiapas depression indicate continuous along strike exposures of a concordant stratigraphy, with only minor changes in dip angle. There are no significant crustal-scale discontinuities between the Chiapas Massif and the central Chiapas depression active during Cenozoic time. This argues against local vertical-axis rotations as the cause of rotation. We also notice that Miocene plutons in coastal Chiapas record concordant directions (Molina-Garza et al., 1994), thus rotation ended prior to about 10 Ma.

The magnetic anisotropy results are consistent with a sedimentary fabric. The bulk susceptibility is low, it is thus possibly influenced by paramagnetic particles. Rock magnetism established the presence of magnetite and hematite. The anisotropy patterns can be interpreted as caused by hydrodynamic imbrication of flakes, that is particles with one short dimension and two similar larger dimensions such as detrital mica or hematite plates. If this is correct, the results indicate fluvial systems flowing from west-southwest to east-northeast. This interpretation is tentative because there is a weak tendency for maximum susceptibility axes to align in the NW-SE direction, that is perpendicular to the inferred shortening direction (Mandujano-Velásquez and Keppie, 2009).

3.1.1. *Explaining a 20° CW rotation (Chiapas Massif) in a sinistral plate boundary zone*

Arcuate folds are a common feature in orthogonally shortened foldbelts, and the shortening direction is generally the “arrow” of the “bow” shape formed by these folds. However, the paleomagnetic data for El Bosque Formation, and hence of the Chiapas Massif basement indenter on which El Bosque rests, indicate about 20° of rotation since the Middle Eocene. Later, we argue rotation occurred predominantly during the Neogene as Chiapanecan orogeny folding progressed. Further, the foldbelt contains numerous sinistral strike slip faults (Fig. 1), and shortening at the SE end of the Sierra de Chiapas Foldbelt is abruptly relayed eastwards by the sinistral Polochic fault system. Thus, the “bow and arrow rule of thumb” may not strictly apply here. Our preferred interpretation of Chiapanecan shortening favors E-W sinistral transpression over orthogonal shortening; hence, the existence of the strike-slip province within the foldbelt (Guzmán-Speziale and Meneses-Rocha, 2000; Pindell and Miranda, 2011). We view the massif as being driven ENE, forming the Chiapas Foldbelt in a bow-wave fashion, where the massif is the boat, and the foldbelt the waves. This could operate with or without rotation of the Chiapas Massif.

Fig. 7 shows three models of rotation for the Chiapas Massif. One is pure vertical-axis rotation about a pole central to the massif (Fig. 7A), which predicts zones of compression in the NW and the SE, with concurrent extension in the SW and the NE. This model is not applicable, because extension is not observed in the NE Chiapas Foldbelt. The second model (Fig. 7B) involves a distant pole of rotation which produces pure ENE translation of the massif; this model is inconsistent with our paleomagnetic data, with no local rotation. The preferred model (Fig. 7C) involves a relatively nearby pole, leading to a combination of translation and rotation. This model incorporates the observed rotation, and is consistent with sinistral strike-slip motion within the Chiapas Foldbelt, as well as along the westernmost Polochic Fault where there is relative motion between the massif and the Yucatán Block (Guzmán-Speziale and Meneses-Rocha, 2000). The closer the pole, the greater the rotation and the lesser the translation. We find, for instance, that a pole near 14°N/92.5°W (with a large error ellipse, and a possibly moving pole, as well) can produce a total linear ENE displacement of about 100 km within the foldbelt, leading to about 60 km of shortening when measured orthogonal to the folds, and keeping the western Polochic Fault essentially transcurrent. In addition, the model of Fig. 7C also is expected to produce a crustal break at the western end of the Chiapas Massif. There, such a break is manifested by the Oaxaca-Río Pinal and Paso de Buques strike slip faults (Fig. 1), and also by the arcuate, presumably sheared, outcrop pattern of the massif and its dislocation from the Mixtequita Massif in the aeromagnetic map of the region (Fig. 8; Servicio Geológico Mexicano, 2008) that we name the Chimalapa deflection.

We conclude that the model of Fig. 7C best explains not only the paleomagnetic data, but also the regional fault and fold patterns (the Tabasco and Campeche provinces to the north are not discussed here). We acknowledge that a clockwise block rotation as presented here within a sinistral transpression zone is not normally expected. Thus, we suspect that something else is occurring, something more significant, than merely internal deformation along a shear system such as that between Chortís and North America. We will expand our scope to identify what this “something else” might be.

Pindell and Miranda (2011) and Villagomez and Pindell (2020) made the case for the eastward migration of hanging-wall uplift in the Middle

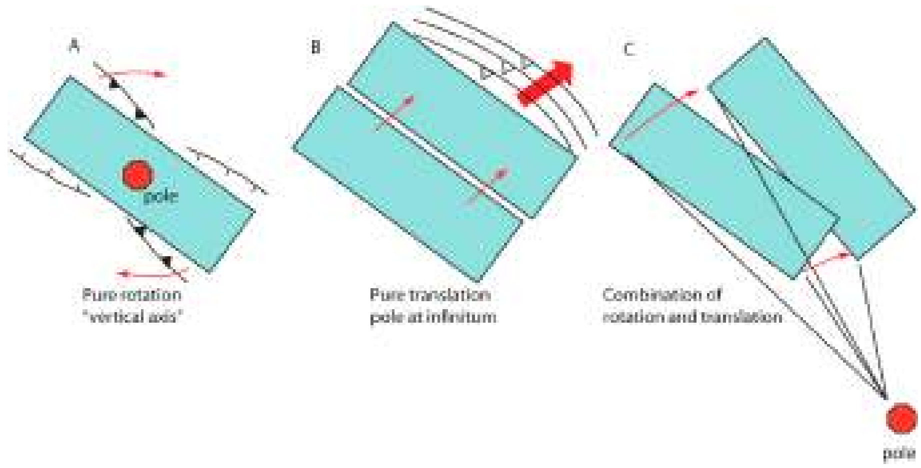

Fig. 7. Model for rotation for the Chiapas Massif, see text for explanation.

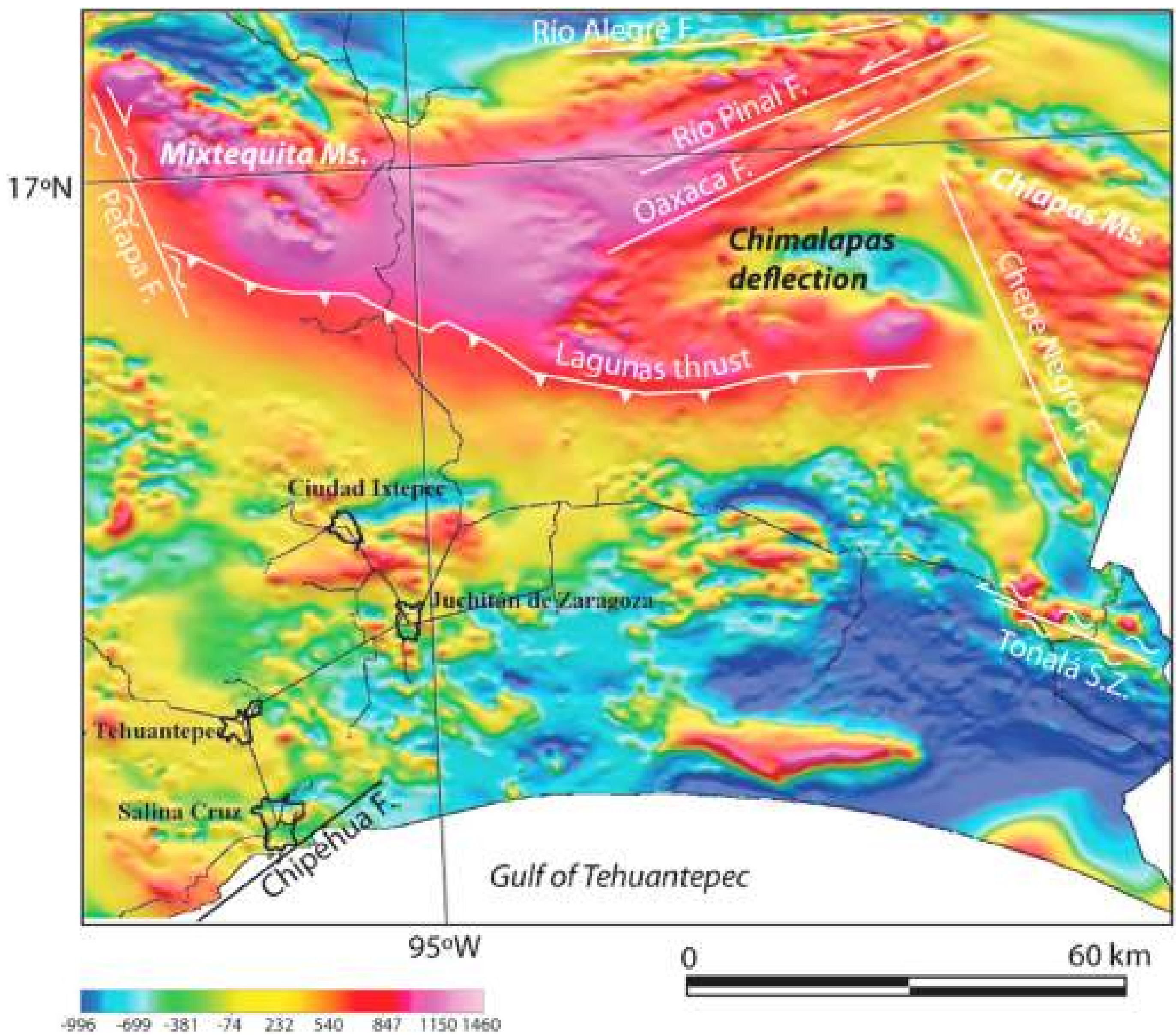

Fig. 8. Aeromagnetic map of eastern Oaxaca, after Servicio Geológico Mexicano (2008).

American trench along the Mexican margin. The cause of uplift was proposed by these authors to be the result of the eastward migration in the inception of subduction of the Cocos Plate in the *wake* of the eastward migrating Chortís Block, rather than to the transcurrent passage of the block itself. This uplift helps to load the Cocos Plate upon initial subduction, leading to the flattening of the upper Benioff Zone. Here, we examine this concept more closely to determine a driving mechanism for CW rotation within a sinistral shear system. Observations pertaining to the question include:

1) The inception of arc magmatism due to subduction of the Cocos Plate has migrated eastward along southern Mexico during Cenozoic time (Damon and Montesions, 1978; Schaaf et al., 1995; Molina Garza et al., 2019b).
2) The flat slab beneath Oaxaca State developed between about 22 and 18 Ma, and involved the migration of arc magmatism from near the present day Oaxaca coast to the Trans-Mexican Volcanic Belt (TMVB) (Ferrari et al., 1999).
3) The flat slab is now expanding into Chiapas, as shown by the arc axis arriving in eastern Tehuantepec at 11 to 9 Ma and then migrating further from 9 Ma to 3 Ma into the Chiapas Foldbelt, where it has been active for Pliocene-Quaternary time (Garduño-Monroy et al., 2015; Molina-Garza et al., 2015).
4) North America-hotspot (mantle) relative motion at the position of Chiapas is WSW-ENE at about 20 mm/yr (e.g., Doubrovine et al., 2012, although other hotspot reference frame papers show slightly different values).
5) The Cocos Plate dives more steeply at the Veracruz Basin and beneath the Gulf of Mexico in the down-dip direction from the flat slab segment (Pardo and Suárez, 1995).
6) The Chortís Block migrates at 20 mm/yr relative to North America (DeMets, 2001), but is essentially fixed in the mantle reference frame with the rest of the Caribbean Plate (Müller et al., 1999).
7) Cocos Plate is too young and buoyant to roll back (Karig-Cordwell et al., 1978) as fast as North America has been moving WSW over the mantle reference frame.
8) Chiapas Massif has undergone its main period of uplift since about 10 Ma (Witt et al., 2012; Villagomez and Pindell, 2020).

Pindell and Miranda (2011) integrated some of these observations with the concepts of subduction zone dynamics of Dewey (1980) to construct their tectonic framework for southern Mexico. Their model can now be supported with additional data and refined by the paleomagnetic data present here:

At 22 Ma, North America was situated 440 km ENE of its present position relative to the regional mantle and to the Chortís Block. The magmatic arc was situated near the present Oaxaca coastline, to the west of the Gulf of Tehuantepec only. There was no flat slab yet, no TMVB yet, and the arc continued to the southeast by passing into the Chortís Block rather than entering Chiapas.

By 17 Ma, North America was situated some 340 km ENE from today's position relative to the regional mantle and the Chortís Block, having migrated WSW by about 100 km since 22 Ma. Because the young Cocos Plate was relatively buoyant, it could not roll back at the same pace as North America's drift across the mantle and the Benioff Zone. Thus, the steep portion of the Benioff Zone remained in place, and North America progressively advanced WSW to produce the flat slab beneath Oaxaca by progressively telescoping onto the Cocos Plate, and forcing the trench position to the WSW with respect to the original Benioff Zone. The magmatic arc recorded this by migrating inland from near the coast to produce magmatism in western Tehuantepec, the Sierra de Juárez, and the eastern and central parts of the TMVB in the late Early Miocene (Ferrari et al., 1999, 2012; Morán-Zenteno et al., 1999). The southeastward continuation of the arc axis passed into Chortís, as before.

By 10 Ma, North America was now roughly 200 km ENE of today's position relative to the mantle and to Chortís. The flat slab in Oaxaca was mostly formed, and the arc had reached the entire TMVB. At this time activity in Los Tuxtlas volcanic field (Fig. 1) was beginning, well-known from 7 Ma onward, and the volcanic arc was also forming along the eastern Gulf of Tehuantepec. Magmatism in eastern Tehuantepec was perhaps facilitated by the Tonalá crustal scale fault serving as a conduit, before continuing southward into Chortís, as before. Within this period (17-10 Ma), the Chiapas Massif completed most of its rotational convergence upon the Yucatán Block as shown by the Chiapanecan folding event recorded beneath the ~10–12 Ma unconformity recognized in seismic profiles (Mandujano-Velásquez and Keppie, 2009). In addition, plutons ca. 10 Ma along the Tonalá Fault do not show rotation (Molina-Garza et al., 1994), indicating that most of the Chiapas Massif's rotation had occurred before 10 Ma. Thus, rotation of the massif seems to be associated with folding in the Chiapas Foldbelt, as expected.

By about 6 Ma, North America's progressive WSW advance across the mantle and the original position of the Benioff Zone continued, such that the flat slab was fully formed in Oaxaca and was now expanding ENE into Chiapas. The arc axis ran from the TMVB to Los Tuxtlas and continued toward the SE, where it was migrating at this time to the northeast beneath Chiapas due to initial slab flattening there. However, there is no known surface expression of arc magmatism in the Chiapas Foldbelt from 9 Ma until about 3 Ma.

Since 3 Ma, arc magmatism has finally broken through the crust and into the Chiapas Foldbelt (Garduño-Monroy et al., 2015) some 150 km to the NE of where it had been at 9 Ma, and where it fills the spatial gap in volcanic activity between Los Tuxtlas and the Central American arc in westernmost Guatemala. The flattening of the slab continues to expand ENE into Chiapas because North America continues to migrate WSW across the regional mantle and Caribbean reference frame. The original steep part of the Benioff Zone, controlled by the mantle reference frame, now underlies Veracruz Basin, directly below the active arc axis, some 440 km ENE of where it was, relative to North America, at 22 Ma. It is North America that has moved primarily, not the arc axis. The plate interface of the entire shallow dipping slab beneath Oaxaca lies above 100 km (Arzate-Flores et al., 2016), such that there is no magmatism there.

This history of flat slab development helps to put the Sierra de Chiapas into its neotectonic perspective and describes a change in geodynamic setting. From 22 to 10-9 Ma, the Chiapas Massif and foldbelt were in a rear-arc position, such that Chiapanecan folding was analogous to Andean foredeep folding. That is, basement-involved shortening behind the arc axis produced a rear-arc fold and thrust belt, and the CW rotation of the massif indicates that overall shortening was greater in the west. This may explain why the 10 Ma unconformity is best developed to the north and northwest in the Chiapas Foldbelt (including the Akal-Reforma trend). An analogous phase of back-arc thrusting has not been recognized in the adjacent Oaxacan segment of the margin. However, such a phase should have occurred earlier in Oaxaca than in Chiapas, and thus part of the apparently "Laramide" shortening history in the western flank of the Veracruz Basin could be related to this process.

Since 9 or 10 Ma the geodynamic setting has been different. The northeastward migration of the arc axis has placed the Chiapas Massif in the forearc position above the flattening slab. Forearc lithospheres can be expected to be brittle down to the plate interface, given that they overlie cold down-going slabs and are thinner than normal due to tapering above the dipping slab. This implies a strengthening of the lithosphere beneath the coastal plain and Chiapas Massif since 9 Ma, as the arc axis migrated inboard. This timing accords with the fastest uplift of the Chiapas Massif, amounting to some 4 km of denudation according to apatite fission track data (Witt et al., 2012; Villagomez and Pindell, 2020). Thus, we suggest that this young uplift of the massif has been ultimately driven by flattening of the Cocos slab under Chiapas, although recall that the flattening is driven by the telescoping of North America onto the Cocos Plate and not by actual elevation of Cocos lithosphere beneath North America as is often portrayed. This telescoping generates tractional coupling at the plate interface (Davis, 1978; Fleitout, 1991), manifested as forearc uplift that is accompanied by strong NE-ward tilting of the massif as shown by active drainage patterns. An additional aspect, however, is that the narrow Pacific coastal plain of Chiapas and the offshore Tehuantepec Shelf, both south of the Tonalá fault zone, did not take part in the strong and rapid uplift of the massif. The intervening Tonalá Fault is responsible for this elevation difference today; since 9 Ma the fault has had a significant northeast-side up component of at least 4–5 km (Molina-Garza et al., 2015; Villagomez and Pindell, 2020). The structural level of the coastal plain and Tehuantepec Shelf has probably been controlled by the arching of the Cocos Plate as it enters the trench and upper part of the Benioff Zone, potentially assisted by tectonic erosion (removal and subduction) of the lower uppermost forearc.

The WSW advance of North America in the mantle reference frame has caused the area of the flat slab to appear, relative to North America, to expand toward the ENE. Thus, the lithosphere beneath the WNW end of Chiapas Massif in the Tehuantepec Isthmus began to engage the Cocos plate interface earlier, with greater overall tractional coupling than the ESE end of the massif. Another way to demonstrate this is to point out that the arc axis from Los Tuxtlas, through the Chiapas Foldbelt, and into western Guatemala, has more of a N–S trend than does the Chiapas Massif, requiring the WNW end of the massif to confront the flat slab earlier. This was also true for the Middle Miocene when we believe most of the CW rotation occurred, and when the arc axis stretched from the TMVB, to Gulf of Tehuantepec, to western Guatemala; indeed, this is especially true if we remove the 20° CW rotation of the massif which reorientates it even more E-W than it is today. The claim that the WWN end of the massif began interaction with the Cocos plate earlier and for a longer time is further supported by the fact that present-day depth contours to the Cocos-North America plate interface are shallower beneath this end of the massif than the ESE end (Guzmán-Speziale and Zúñiga, 2016). With a longer and more intense period of tractional coupling, it follows that the crust at the WNW end of the massif should have shortened more than the crust to the ESE. Hence, the massif has rotated CW, despite being situated within the North America-Caribbean sinistral plate boundary.

4. Discussion

The model outlined herein hints at two distinct phases of Neogene structural evolution for the Chiapas Foldbelt. The first involved Middle Miocene rotational basement shortening of the Chiapas Massif, driving the folds of the foldbelt and the Akal-Reforma Trend ahead of it, and producing the 10 Ma unconformity in the north and northwest (Graham et al., 2020). The second involved rapid Late Miocene to Recent non-rotational uplift and NE-ward tilting of the Chiapas Massif, accompanied by sinistral E-W displacements along faults within the Chiapas Foldbelt that cut and slightly offset the Middle Miocene folds (Meneses-Rocha, 2001). Pindell and Miranda (2011, their Fig. 1) portrayed main structures of this second phase, which are distributed over a broad area including the initiation of movement along the Polochic Fault (Obrist-Farner et al., 2020). Today, the entire Chiapas-Guatemala setting is aptly considered as a widely distributed plate boundary zone.

There may be an additional consideration to refine our model. The Tehuantepec Ridge is a fracture zone in the Cocos plate that separates a 16 Ma oceanic crust, to the west, from a 26 Ma crust to the east (Nixon 1982). The ridge reached the trench and currently subducts under Chiapas. Guzmán-Speziale and Zúñiga (2016) find a shallow-dipping subducting Cocos plate underneath North America and a steeper-dipping slab under the Caribbean plate, with a smooth transition between them. Different subduction regimes had been previously recognized by Couch and Woodcock (1981) across the Tehuantepec ridge. Furthermore, the subducted Cocos slab dips at low angles of 15–30° to the west of the Tehuantepec Ridge (Pardo and Suárez 1995; Rebollar et al., 1999; Ponce et al., 1992) and 35–45° to the east (Rebollar et al., 1999; Guzmán-Speziale and Zúñiga, 2016). The different lithospheres on either side of the Tehuantepec ridge thus may have facilitated or enhanced flattening of a more buoyant slab of oceanic lithosphere to the west of it.

5. Conclusions

The ChRM in the Eocene El Bosque Formation in the Chiapas central depression, in southern Mexico, is a dual polarity magnetization carried by hematite and magnetite; pigmentary hematite is the dominant remanence carrier. The north-northeast (or south-southwest) directed magnetization is discordant with respect to the expected direction calculated from the North America craton, indicating a clockwise rotation of $+22.4^\circ \pm 6.1^\circ$. We propose a model to explain rotation where the Miocene eastward migration of the North America-Cocos-Caribean triple plate junction, and concurrent slab-flattening as the North America plate telescoped over Cocos, caused differential basal traction to act on the lithosphere of the Chiapas Massif in its WNW end with respect to its ESE end. This in turn caused clockwise rotation of the Chiapas Massif, basement of the Mesozoic-Cenozoic succession of the Chiapas central depression. Rotation of the Chiapas Massif after deposition of El Bosque Formation, but prior to emplacement of late Miocene plutons in coastal Chiapas, may thus explain formation of the Sierra Chiapas foldbelt if the massif acted as an indenter.

Author contributions

Roberto Molina Garza: Conceptualization, Methodology, Data curation, Writing- Original draft preparation. **James Pindell**: Writing-Reviewing and Editing, Visualization, Investigation. **Paola Catalina**: Field and laboratory work, Methodology, Data curation.

Declaration of competing interest

The authors declare that they have no known competing financial interests or personal relationships that could have appeared to influence the work reported in this paper.

Acknowledgements

This research was supported by the Tectonic Analysis-UNAM consortium for studying Cordilleran Mexico and the Gulf of Mexico (Phase 2); we thank BHP, Chevron, ConocoPhillips, ENI, Equinor, ExxonMobil, Hess, and Shell for sponsorship of this program. We also thank Daniel Serrano and Pedro V. Paiva for assistance in the field. We thank the comments of the journal's editor and anonymous reviewers.

Appendix A. Supplementary data

Supplementary data to this article can be found online at https://doi.org/10.1016/j.jsames.2020.102932.

References

Arzate-Flores, J.A., Molina-Garza, R.S., Corbo-Camargo, F., Máquez-Ramírez, V., 2016. Low angle contact between the Oaxaca and Juárez terranes deduced from magnetotelluric data. Pure Appl. Geophys. https://doi.org/10.1007/s00024-016-1295-y.

Bailey, R.C., Halls, H.C., 1984. Estimate of confidence in paleomagnetic directions derived from mixed remagnetization circle and direct observational data. J. Geophys. 54, 174–182.

Blair, T.C., 1987. Tectonic and hydrologic controls on cyclic alluvial fan, fluvial, and lacustrine rift-basin sedimentation, Jurassic–Lowermost Cretaceous Todos Santos Formation, Chiapas. Mexico. J. Sediment. Pet 57, 845–862.

Chávez-Valois, V.M., 1997. Análisis estructural del área Lacantún, porción oriental de la Sierra de Chiapas. Bol. Asoc. Mex. Geol. Pet. 46 (1), 72–92.

Couch, R., Woodcock, S., 1981. Gravity and structure of the continental margins of southwestern Mexico and northwestern Guatemala. J. Geophys. Res. https://doi.org/10.1029/JB086iB03p01829.

Cros, O., Michaud, F., Fourcade, E., Fleury, J.J., 1998. Sedimentological evolution of the Cretaceous carbonate platform of Chiapas (Mexico). J. South Am. Earth Sci. 11, 311–332.
Damon, P.E., Montesions, E., 1978. Late Cenozoic volcanism and metallogenesis over an active Benioff zone in Chiapas, Mexico. Ariz. Geol. Soc. Digest 11, 155–168.
Davis, G.F., 1978. The roles of boundary friction, basal shear stress and deep mantle convection in plate tectonics. Geophys. Res. Lett. https://doi.org/10.1029/GL005i003p00161.
DeMets, C., 2001. A new estimate for present-day Cocos-Caribbean plate motion: implications for slip along the Central American volcanic arc. Geophysical Research Letters 4043–4046. https://doi.org/10.1029/2001GL013518 v. 28.
Dengo, G., 1969. Problems of tectonic relations between Central America and the Caribbean. Trans. Gulf Coast Assoc. Geol. Soc. 19, 311–320.
Dewey, J.F., 1980. Episodicity, sequence and style at convergent plate boundaries. Geol. Assoc. Can. Spec. Pap. 20, 553–573.
Doubrovine, P.V., Steinberger, B., Torsvik, T.H., 2012. Absolute plate motions in a reference frame defined by moving hot spots in the Pacific, Atlantic, and Indian oceans. J. Geophys. Res. 117, B09101. https://doi.org/10.1029/2011JB009072.
Enkin, R.J., 2003. The direction^correction tilt test: an all-purpose tilt/fold test for paleomagnetic studies. Earth Planet Sci. Lett. 212, 151–166.
Ferrari, L., López-Martínez, M., Aguirre-Díaz, G., Carrasco-Núñez, G., 1999. Space-time patterns of cenozoic arc volcanism in central Mexico: from the sierra Madre Occidental to the Mexican volcanic belt. Geology 27, 303–306.
Ferrari, L., Orozco-Esquivel, T., Manea, V., Manea, M., 2012. The dynamic history of the Trans-Mexican Volcanic Belt and the Mexico subduction zone. Tectonophysics 522–523, 122–149.
Ferrusquía-Villafranca, I., Appelgate, S.P., Espinosa-Arrubarrena, L., 2000. First Paleogene selachifauna of the middle American-Caribbean-Antillean region, La Mesa de Copoya, west central Chiapas – geologic setting. Rev. Mex. Ciencias Geol. 17, 1–23.
Fisher, R.A., 1953. Dispersion on a sphere. Proc. Roy. Soc. Lond. A 217, 295–305.
Fleitout, L., 1991. The sources of lithosperica tectonic stresses. In: Whitmarsh, R.B., Bott, M.H.P., Fairhead, J.B., Kusznir, N.J. (Eds.), Tectonic Stress in the Lithosphere. Philosophical Transactions of the Royal Society London A, vol. 337, pp. 73–81.
Fourcade, E., Piccioni, L., Escribá, J., Rosselod, E., 1999. Cretaceous stratigraphy and palaeoenvironments of the southern petén basin, Guatemala. Cretac. Res. 20, 793–811.
Garcia-Molina, G., 1995. Structural evolution of SE Mexico (Chiapas-Tabasco Campeche) offshore and onshore. Ph. D. thesis. Rice University, p. 161.
Garduño-Monroy, V.H., Macias, J.L., Molina-Garza, R.S., 2015. Geodynamic setting and pre-volcanic geology of active volcanism in Chiapas. In: Scolamacchia, T., Macías, J. L. (Eds.), Active Volcanoes of Chiapas (Mexico): El Chichón and Tacaná, Active Volcanoes of the World, p. 1. https://doi.org/10.1007/978-3-642-25890-9. Springer-Verlag Berlin Heidelberg.
Godínez-Urban, A., Lawton, T.F., Molina-Garza, R.S., Iriondo, A., Weber, B., López-Martínez, M., 2011. The Jurassic volcanic and sedimentary rocks of La Silla and Todos Santos formations, Chiapas: record of Nazas arc magmatism and rift basin formation prior to opening of the Gulf of Mexico. Geosphere 7, 121–144.
Graham, R., Pindell, J., Villagomez, D., Molina-Garza, R.S., Granath, J., Sierra-Rojas, M. I., 2020. Structural sections through the cuicateco-veracruz and Chiapas. Geological Society, London, Special Publications 504. https://doi.org/10.1144/SP504-2020-70.
Guzmán-Speziale, M., Meneses-Rocha, J.J., 2000. The Noth America-Caribbean plate boundary best of the Motagua- Polochic fault system: a fault jog in Southeastern Mexico. J. South Am. Earth Sci. 13, 459–468.
Guzmán-Speziale, M., Zúñiga, F.R., 2016. Differences and similarities in the Cocos–North America and Cocos–Caribbean convergence, as revealed by seismic moment tensors. J. S. Am. Earth Sci. 71, 296–308.
Islas-Tenorio, J.J., Sáenz-Pita, M.R., Beltrán-Castillo, D.H., Valdés-Vigil, J.E., 2005. Carta geológico-minera tenosique E15-9, escala 1:250,000: pachuca, hidalgo, méxico, Servicio Geológico Mexicano, informe, p. 58.
Karig-Cordwell, D.E., Moore, G.F., Moore, D.G., 1978. Late Cenozoic subduction and continental margin truncation along the Middle America Trench. Geol. Soc. Am. Bull. 89, 265–276.
Keppie, D.F., Hynes, A.J., Lee, J.K.W., Norman, M., 2012. Oligocene-Miocene back-thrusting in southern Mexico linked to the rapid subduction erosion of a large forearc block. Tectonics 31, TC2008,. https://doi.org/10.1029/2011TC002976.
Kirschvink, J.L., 1980. The least-squares line and plane and the analysis of paleomagnetic data: examples from Siberia and Morroco. Geophys. J. Roy. Astr. Soc. 62, 699–718.
Mandujano-Velásquez, J.J., 1996. Cuatro megasecuencias de evolución litoestratigráfica en la sierra de Chiapas. Bol. Asoc. Mex. Geol. Petrol 44 (1), 44–60.
Mandujano-Velásquez, J.J., Keppie, J.D., 2009. Middle Miocene Chiapas Fold and thrust belt of Mexico: a result of collision of the Tehuantepec transform/Ridge with the Middle America trench. In: Murphy, J.B., Keppie, J.D., Hynes, A.J. (Eds.), Ancient Orogens and Modern Analogues. Geological Society London Special Publications, vol. 327, pp. 55–69.
McFadden, P.L., McElhinny, M.W., 1990. Classification of the reversal test in palaeomagnetism. Geophys. J. Int. 103, 725–729.
Meneses-Rocha, J.J., 1985. Tectonic evolution of the strike-slip fault province of Chiapas. Mexico [M.S. Thesis]. University of Texas at Austin, Austin, TX, p. 315.
Meneses-Rocha, J.J., 2001. Tectonic evolution of the Ixtapa Graben, an example of a strike-slip basin of southeastern Mexico: implications for regional petroleum systems. In: Bartolini, C., Buffler, R.T., Cantú-Chapa, A. (Eds.), The Western Gulf of Mexico Basin: Tectonics, Sedimentary Basins and Petroleum Systems: Am. Assoc. Petrol. Geol. Mem, vol. 75, pp. 183–216.
Molina-Garza, R.S., Urrutia-Fucugauchi, J., Van der Voo, R., 1994. Concordant paleomagnetic directions from the Tehuantepec Isthmus: constraints on the Neogene evolution of the north America-Caribbean Plate boundary. Tectonophysics 235, 339–346.
Discussion of: Ortega-Flores et al.. (2018) Molina Garza, R.S., Pindell, J., Villagomez, D., 2019. Provenance analysis of oligocene sandstone from the cerro pelón area, southern Gulf of Mexico. Int. Geol. Rev.. https://doi.org/10.1080/00206814.2019.1616620.
Molina-Garza, R.S., Geissman, J.W., Wawtzyniec, T.F., Peña Alonso, T.A., Iriondo, A., Weber, B., Aranda-García, J.J., 2015. Geology of the coastal Chiapas (Mexico) Miocene plutons and the Tonalá shear zone: syntectonic emplacement and rapid exhumation during sinistral transpression. Lithosphere 10.1130/L409.1 (7), 257–274.
Molina-Garza, R., van Hinsbergen, D.J.J., Boschman, L.M., Rogers, R.D., Ganerød, M., 2019. Large-scale rotations of the Chortís Block (Honduras) at the southern termination of the Laramide flat slab. Tectonophysics 760, 36–57. https://doi.org/10.1016/j.tecto.2017.11.026.
Molina-Garza, R.S., Lawton, T.F., Barboza Gudiño, J.R., Sierra-Rojas, M.I., Figueroa Guadarrama, A., Pindell, J., 2020. Geochronology and correlation of the Todos Santos Group, western Veracruz and eastern Oaxaca states. In: Martens, U., Molina Garza, R.S. (Eds.), Southern and Central Mexico: Basement Framework, Tectonic Evolution, and Provenance of Mesozoic–Cenozoic Basins:Geol. Soc. Am. Spec. Implications for regional stratigraphic relations and the rift history of the Gulf of Mexico, Mexico, p. 546. https://doi.org/10.1130/2019.2546(06).
Moran-Zenteno, D.J., Tolson, G., Martinez-Serrano, R.G., Martiny, B., Schaaf, P., Silva-Romo, G., Macias Romo, C., Alba-Aldave, L., Hernandez-Bernal, M.S., Solis Pichardo, G.N., 1999. Tertiary arc-magmatism of the Sierra Madre del Sur, Mexico, and its transition to the volcanic activity of the Trans-Mexican Volcanic Belt. J. South Am. Earth Sci. 12, 513–535.
Muller, R.D., Royer, J.Y., Cande, S.C., Roest, W.R., Maschenkov, S., 1999. New Constraints on the Late Cretaceous/tertiary Plate Tectonic Evolution of the Caribbean. In: Mann, P. (Ed.), Caribbean Basins, Sedimentary Basins of the World 4. Elsevier Science, London, pp. 33–59.
Nixon, G.T., 1982. The relationship between Quaternary volcanism in central Mexico and the seismicity and structure of subducted ocean lithosphere. Geol. Soc. Am. Bull. 93 (6), 514–523.
Obrist-Farner, J., Eckert, A., Locmelis, M., Crowley, J.L., Mota-Vidaure, B., Lodolo, E., Rosenfeld, J., Duarte, E., 2020. The role of the Polochic fault as part of the north American and Caribbean plate boundary: insights from the infill of the lake izabal basin. Basin Res. 1–18. https://doi.org/10.1111/bre.12431, 00.
Pardo, M., Suárez, G., 1995. Shape of the subducted Rivera and Cocos plates in southern Mexico: seismic and tectonic implications. J. Geophys. Res. 100, 12357–12373.
Pindell, J., Dewey, J.F., 1982. Permo-Triassic reconstruction of western Pangea and the evolution of the Gulf of Mexico/Caribbean region. Tectonics. https://doi.org/10.1029/TC001i002p00179.
Pindell, J., Miranda, E., 2011. Linked kinematic histories of the macuspana, akal-reforma, comalcalco, and deepwater Campeche basin tectonic elements. southern Gulf of Mexico: Gulf coast association of geological societies transactions 61, 353–361.
Pindell, J.L., Cande, S.C., Pitman, W.C., Rowley, D.R., Dewey, J.F., Labrecque, J., Haxby, W., 1988. Pindell A plate-kinematic framework for models of Caribbean evolution. Tectonophysics 155, (1–4), 121–138.
Ponce, L., Gaulon, R., Suárez, G., Lomas, E., 1992. Geometry and state of stress of the downgoing Cocos plate in the Isthmus of Tehuantepec, Mexico. Geophys. Res. Lett. https://doi.org/10.1029/92GL00437.
Quezada-Muñetón, J.M., 1987. El Cretácico Medio-Superior y el límite Cretácico Superior-Terciario Inferior en la Sierra de Chiapas. Bol. Asoc. Mex. Geol. Petrol. 39 (1), 3–98.
Ratschbacher, L., Franz, L., Min, M., Bachmann, R., Martens, U., Stanek, K., Stübner, K., Nelson, B.K., Herrmann, U., Weber, B., López-Martínez, M., Jonckheere, R., Sperner, B., Tichomirowa, M., Mcwilliams, M.O., Gordon, M., Meschede, M., Bock, P., 2009. the North American-Caribbean plate boundary in Mexico-Guatemala-Honduras. Geol. Soc. London Spec. Pub. 328, 219–293.
Rebollar, C.J., Espíndola, V.H., Uribe, A., Mendoza, A., Pérez, V.A., 1999. Distribution of stresses and geometry of the wadati–benioff zone under Chiapas, Mexico. Geophysical Internat 38, 95–106.
Rosenfeld, J.H., 1993. Sedimentary rocks of the santa cruz ophiolite, Guatemala – a proto-caribbean history. In: Pindell, J.L., Perkins, R.F. (Eds.), Transactions of the 13th Annual GCSSEPM Research Conference: Mesozoic and Early Cenozoic Development of the Gulf of Mexico and Caribbean Region, pp. 173–180. Houston, TX.
Schaaf, P., Morán-Zenteno, D., Hernández-Bernal, M., Solís-Pichardo, G., Tolson, G., Köhler, H., 1995. Paleogene continental margin truncation in southwestern Mexico: geochronological evidence. Tectonics 14 (5), 1339–1350.
Servicio Geológico Mexicano, 2005. Carta Geológico minera Tuxtla Gutiérrez, oaxaca-chiapas, secretaría de Economía, pachuca, hidalgo, méxico. 1 sheet 1, 250,000.
Servicio Geológico Mexicano, 2008. Carta Magnética del Estado de Oaxaca, 1 sheet, 1: 500,000 (Pachuca, Hidalgo).
Tauxe, L., Kent, D.V., 2004. A simplified statistical model for the geomagnetic field and the detection of shallow bias in paleomagnetic inclinations: was the ancient magnetic field dipolar? In: Channell, J.E.T., Kent, D., Lowrie, W., Meert, J.G. (Eds.), Timescales of the Paleomagnetic Field. : Geophysical Monograph, 145. AGU, pp. 101–117. Washington, D.C.
Torsvik, T., Van der Voo, R., Preeden, U., Niocaill, M.C., Steinberger, B., Doubrovine, P. V., Van Hinsbergen, D.J.J., Domeier, M., Giana, C., Tohver, E., Meert, J.,

McCausland, P.J.A., Cocks, R., 2012. Phanerozoic polar wander, palaeogeograghy and dynamics. Earth Sci. Rev. 114, 325–368.

Vega, F.J., Nyborg, T., Coutiño, M.A., Hernández-Monzón, O., 2008. Review and additions to the eoceno decapod Crustacea from Chiapas, Mexico. Bull. Mizunami Foss. Mus. 34, 51–71.

Villagomez, D., Pindell, J., 2020. Cooling and uplift history of the Chiapas Massif and its influence on sedimentation and deformation in the adjacent Sierra.

Vinson, G.L., 1962. Upper cretaceous and tertiary stratigraphy of Guatemala. Bull. Am. Assoc. Petrol. Geol. 62 (4), 425–456.

Witt, C., Rangin, C., Andreani, L., Olaez, N., Martínez, J., 2012. The transpressive left-lateral Sierra Madre de Chiapas and its buried front in the Tabasco plain (southern Mexico). J. Geol. Soc. Lond 169, 143–155. https://doi.org/10.1144/0016-76492011-024.

Zijderveld, J.D.A., 1967. The natural remanent magnetization of the exeter volcanic traps (permian, europe). Tectonophysics 4, 121–153.